

# Measuring the intensity and position of a pA electron beam with resonant cavities

Thorsten R. Pusch,<sup>\*</sup> F. Frommberger, W. C. A. Hillert, and B. Neff

*ELSA, Physics Institute, University of Bonn, 53115 Bonn, Germany*

(Received 27 April 2012; published 14 November 2012)

In order to continuously monitor the intensity and position of an electron beam of a few hundred pA, a system of resonant cavities has been set up. The current measurement relies on signals of a few fW power extracted out of a cylindrical resonator, excited at its  $\text{TM}_{010}$  mode. The demodulated cavity pickup signal allows the reconstruction of the beam current with a precision of a few pA. For beam position measurements, we designed two resonators, one each for the horizontal and vertical plane. They are excited at their  $\text{TM}_{110}$  dipole modes, the signal strength vanishing with the beam passing on their symmetry axis. Commercial digital lock-in amplifiers perform a phase-sensitive detection of the position signals, separating them from background noise. A frequency mixing scheme was applied to transform the signals into the passband of the amplifiers. Great care was taken to prevent cross talk by using special shielding. With these techniques, a relative beam position resolution of 50  $\mu\text{m}$  was achieved. The position readings are sampled with a maximum rate of 9 Hz. A standard PC is used to read out the lock-in amplifiers. It transfers the measured raw data as well as processed values to the accelerator control system for graphical display.

DOI: 10.1103/PhysRevSTAB.15.112801

PACS numbers: 41.85.Qg, 29.27.Fh, 84.40.Dc, 07.50.Qx

## I. INTRODUCTION

The on-line monitoring of electron beam intensity and orbit is mission critical for the operation of the fixed target experimental setup at ELSA (Bonn, Germany) [1], especially when using a polarized beam. Such beam diagnostics allows one to optimize the settings of the guide field magnets, and may later be used in an automatized feedback loop to stabilize the beam orbit. A diagnostic scheme based on resonant cavities has been investigated, considering beam currents of a few hundred pA while aiming for a position resolution down to few tenths of a millimeter. Continuous surveillance of the beam parameters requires the diagnostical method not to deteriorate the beam quality. While a resonant cavity may exert a negligible influence on the passing electron bunches, it will give a sufficiently large, detectable beam-related signal via a coupling device.

At the accelerator facility ELSA, an electron beam of a few hundred pA is extracted from a storage ring via slow resonance extraction over a periodically recurring phase of a few seconds. Between extractions, roughly one second is needed for the storage ring to be refilled. A dipole magnet fork in the external beam line allows one to send the electron beam spill into one of the two experimental areas dedicated to hadron physics experiments, namely CBELSA/TAPS and BGO-OD [2,3]. There, bunches typically carrying some five electrons each are sent onto a radiator target. Because of the bunch repetition rate of

about 500 MHz and a feedback loop stabilizing the beam current, a quasi-cw beam can be offered during extraction. The experimental setups both rely on bremsstrahlung photons emitted by the electrons in the radiator. In its immediate proximity, our cavity-based position detection system of the primary beam is implemented. The beam current is measured upstream, in close vicinity of the last extraction septum of the storage ring.

A full measurement setup consists of one intensity and two position cavities, each of the latter being sensitive only in one spatial direction. The signal coupled out of a position cavity via an antenna is preamplified and mixed down to a frequency within the passband of a lock-in amplifier. Similar measurement systems based on this principle and designed for use in the nA regime have been conceived at CEBAF (TJNAF) and at MAMI (University of Mainz, Germany) [4,5].

In the implementation presented here, cross talk and other unwanted signal components could be eliminated to a satisfactory degree by appropriate filtering and shielding. Special care has been taken to minimize noise in the circuitry, which is the limiting factor to the measurement resolution. In the present setup, the beam's position is measured down to roughly half a tenth of a millimeter. The position signals have to be normalized based on the beam current, which is measured with a few pA precision. In routine operation, the beam position can be measured at beam currents well below 100 pA.

## II. RESONANT CAVITIES IN BEAM DIAGNOSTICS

### A. Measurement principle

Any closed hollow metal recipient has a—in principle infinite—set of rf resonant modes, which are defined by the

<sup>\*</sup>t.pusch@uni-bonn.de

Published by the American Physical Society under the terms of the [Creative Commons Attribution 3.0 License](#). Further distribution of this work must maintain attribution to the author(s) and the published article's title, journal citation, and DOI.

boundaries of the conduction walls, i.e. the geometry of the resonator. For cylindrically symmetric resonant structures, as typically used in accelerator applications, these so-called eigenmodes are often characterized by the field component constrained to the transverse plane. The transverse magnetic modes (TM) are of particular interest for cavities applied for accelerator diagnostics, as the electric field vector is aligned with the longitudinal  $z$  axis, i.e., the TM modes couple to the beam. Of course, beam port openings in the resonant structure have to be provided, to allow for its passage.

The eigenmodes can be characterized by three integer numbers ( $m, n, p$ ), each approximately corresponding to the number of half oscillations in each spatial dimension. In the most simplistic case of a perfectly evacuated “pillbox” cylinder of length  $L$  and radius  $R$ , the eigenfrequencies are given by

$$\nu_{mnp} = \frac{1}{2\pi\sqrt{\mu_0\epsilon_0}} \sqrt{\left(\frac{j_{mn}}{R}\right)^2 + \left(\frac{p\pi}{L}\right)^2}, \quad (1)$$

where  $j_{mn}$  denotes the  $n$ th root of the  $m$ th order Bessel function. A bunched beam passing the resonator may excite some of the TM modes, and some energy of the beam is lost into the slowly decaying fields of the cavity. A design optimization of the cavity geometry will align a preferred TM eigenmode to the stimulus signal, which basically is a frequency harmonic of the bunch frequency. This will ensure a positive pileup of the resonant field energy in the cavity during the bunch passage, therefore an optimal coupling to the beam.

The eigenmodes in cylindrical structures are further characterized by the rotational symmetry: monopole modes ( $m = 0$ ), dipole modes ( $m = 1$ ), quadrupole modes ( $m = 2$ ), etc. The field distribution of the lowest monopole mode  $\text{TM}_{010}$  lends itself to current measurements, the lowest dipole mode  $\text{TM}_{110}$  is preferred for the position detection. Figure 1 illustrates the latter as an example.

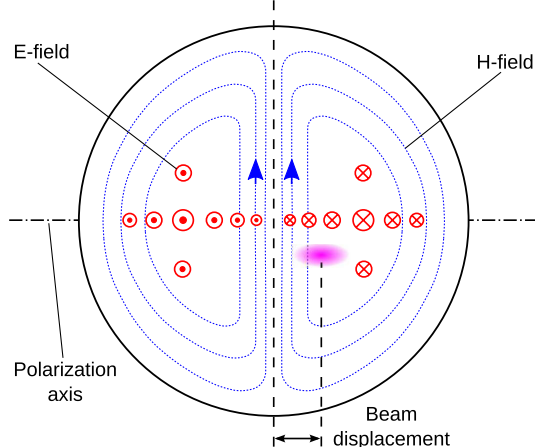


FIG. 1. A simplified, schematic view of the  $\text{TM}_{110}$  dipole mode field distribution, as used in beam position measurements.

Finally, to extract an electrical signal from the beam excited resonator, a simple pin (E-field) or loop (H-field) antenna is used to feed a 50 Ohm coaxial port. Location and orientation of this antenna have to be optimized for the best coupling performance, while suppressing unwanted mode signals.

## B. Signal power

The power of the signal coupled out of a resonant cavity is essentially given by [6]

$$P = R_s I^2 B^2 \frac{\kappa}{(1 + \kappa)^2} \cos^2 \phi. \quad (2)$$

It will depend on both, on properties of the beam (beam current  $I$ , bunch factor  $B$ ) and of the resonator itself (position-dependent shunt impedance  $R_s$ , coupling coefficient  $\kappa$ ). In order to allow for a detuning of the cavities and the ensuing nonresonant excitation to be accounted for, the phase factor  $\cos^2 \phi$  has been added.

## 1. Beam properties

The power of the extracted signal notably depends on the beam current  $I$  modified by the *bunch factor*  $B$ . By the latter, the influence of the width of the longitudinal charge distribution of a particle bunch is factored into the equation. In case of electrons, the bunches essentially feature a Gaussian shape, leading to an analogous envelope of the signal spectrum when evaluating the Fourier transform of the linear charge density of an infinite bunch train [7,8].

For a cavity to be excited at a given eigenfrequency  $\nu_0$ , the bunch factor can be expressed by the standard deviation  $\sigma_\tau$  of a Gaussian, describing the charge density of an electron bunch in time domain:

$$B(\nu_0, \sigma_\tau) = e^{-2\pi^2\nu_0^2\sigma_\tau^2}. \quad (3)$$

Bunches of greater longitudinal expansion will lead to a narrower Gaussian envelope in the frequency domain, and thus to reduced excitation strength. For typical beam energies at the ELSA facility ranging 2–3 GeV, and appropriate accelerating voltages,  $\sigma_\tau$  is typically 40–90 ps. The measurements shown in the following are mostly based on a bunch factor of about 0.8. The respective diagnostic cavities are tuned to roughly 1.5 GHz, the third harmonic of the accelerator rf set to 499.67 MHz. The latter corresponds to the bunch repetition rate during routine operation.

## 2. Cavity properties

In the vicinity of one of its eigenfrequencies, a resonant cavity can be characterized by a parallel LC oscillator circuit. At resonance, the losses of the field energy, e.g., due to the finite conductivity of the walls, can be quantized by the so-called unloaded quality factor  $Q_0$ , i.e., the  $Q$  value of the resonator without external coupling. The

coupling constant  $\kappa$  in (2) expresses the extraction of some stored field energy to a measurement port, typically a 50 Ohm coaxial cable. These external losses, together with  $Q_0$ , will define the shape of the resonant curve in the frequency domain.

In case the cavity eigenfrequency  $\nu_0$  is slightly mistuned with respect to the excitation signal, the resonator is operated by  $\Delta\nu$  off center the resonant curve, which gives a reduction in measurement signal power. In (2), this fact is accounted for by the phase difference  $\phi$  between excitation signal and circuit oscillations. The formalism of LC circuits yields

$$\cos^2\phi = \frac{1}{1 + 4Q^2(\frac{\Delta\nu}{\nu_0})^2} \quad (4)$$

as an expression for the phase factor, with the parameter  $Q$  representing the loaded quality factor accounting for the external losses. It is related to the unloaded one by  $Q_0 = (1 + \kappa)Q$ , which is referred to in the following when discussing fundamental cavity properties.

In order to specify the resistance a given resonator represents to a passing beam current, the *shunt impedance*  $R_s$  associated with an eigenmode can be defined as follows [9]:

$$R_s(r, \varphi) = \frac{1}{2P_{\text{loss}}} \left| \int_0^L E_z(r, \varphi, z) e^{i[\omega_0(z/c) + \phi_0]} dz \right|^2. \quad (5)$$

The usage of the cylindrical coordinates  $(r, \varphi, z)$  reflects the choice of geometries which are typical for resonator structures used in accelerators, including their beam pipe extensions. Each cavity's symmetry axis is assumed to be aligned with the  $z$  direction. The above definition essentially compares the potential difference a particle passing through a cavity of length  $L$  will cross to the Ohmic power losses of the wall currents related to the field oscillations ( $\omega_0$ ).

Electron beams accelerated to energies in the GeV range are highly relativistic, their particles travel very close to the speed of light. The time dependency of the field is reparametrized accordingly by  $z/c$ . In general, the result of the integration in (5) will vary according to the phase  $\phi_0$  of the field oscillations at which any individual particle enters the resonator. Because of the inhomogeneous field distribution of the modes, the integrated field seen by the electrons will depend on the specific path they travel through the cavity.

In the present case, we assume the beam path to be always parallel to the  $z$  axis the electrical field of the first basic eigenmodes is aligned with. This assumption is validated by other diagnostic means at our disposal permitting to judge the beam's alignment. Under this condition, the shunt impedance essentially depends on the transverse beam coordinates  $r$  and  $\varphi$ . According to the beam parameter to be measured, a specific eigenmode either with a low or a high field variation in the region of interest will be chosen.

### C. Suitable eigenmodes

The dominant frequencies at which a particle beam may excite cavity resonances are determined by its time structure, namely, by the bunch frequency and the related harmonics. The resonant frequency of the eigenmode of interest, typically a low TM mode which has a strong shunt impedance, has to be matched with one of these. Once a general cavity geometry has been chosen, its specific dimensions have to be optimized. For practical reasons, e.g., precision manufacturing on a lathe, simple cylindrical geometries are preferred.

Regardless of the field distribution chosen, the strength of the signal coupled out of a resonant cavity as given by (2) will inherently depend on the beam current  $I$ . When only the latter has to be evaluated, the TM<sub>010</sub> mode proves to be the best choice. In the idealized case of a simplistic *pillbox* cavity, an analytical analysis reveals it to feature a purely longitudinal electrical field component [7]. It is given by

$$E_z(r, \varphi, t) = E_0 J_0(\frac{j_{01}}{R} r) e^{i\omega_0}, \quad (6)$$

and has to vanish at the conducting cavity rim. The radial dependency of the  $J_0$  Bessel function is rescaled accordingly by the ratio of its first root  $j_{01}$  and the cavity radius  $R$ . Figure 2(a) shows a numerical simulation of the electric field distribution. The maximum field value is attained on the symmetry axis in whose vicinity the particle beam will pass by. The field strength as given by (6) only gradually declines in the central region, following the  $J_0$  Bessel function. Thus, the measurement is only slightly dependent on beam displacements.

When trying to deduct the beam's position from a cavity signal, the electric field of the TM<sub>110</sub> mode, depicted in Fig. 2(b), suits best the requirements. As the analytical result

$$E_z(r, \varphi, t) = E_0 J_1(\frac{j_{11}}{R} r) \cos(\varphi) e^{i\omega_0} \quad (7)$$

suggests, the modulus of its longitudinal electrical field component follows the  $J_1$  Bessel function. It rises almost linearly from zero value when leaving the symmetry axis of

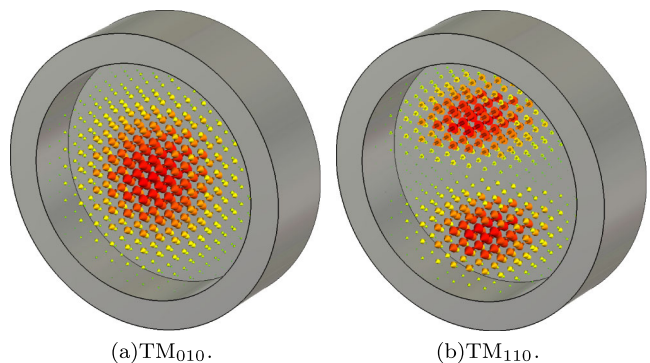


FIG. 2. Distribution of the electric field in a pillbox cavity for two basic modes, as calculated by CST MICROWAVE STUDIO®.

the resonator. This dependency translates to the signal voltage measured after demodulation. The approximation holds true for small displacements not exceeding roughly the first quarter of the cavity's radius, the deviation can then be calculated to remain below 5%. If not extending beyond this central region, the transversal dimension of the beam has a negligible effect on the measured signal due to this linearity, assuming a reasonable symmetry of the charge density.

Because of the dipole structure exhibited by the mode, the fields as shown in Fig. 2(b) will only vary perceptibly along the polarization axis. By design details, it should be aligned with the horizontal or vertical axis. In principle, the circular symmetry would allow for other mode orientations to be excited. In order to avoid cross talk and tuning issues, their respective resonance frequencies are detuned in the present setup. Therefore two resonators with orthogonal dipole mode polarizations have to be provided for the beam position measurement.

As the dipole mode signal magnitude has no information about the half plane, its phase has to be compared to a reference signal, e.g., the accelerator rf. It will differ by 180 degrees depending on whether the beam is displaced up or down, respectively right or left.

#### D. Cavity design

While a simple cavity geometry can be estimated based on analytical approximations, the effects of specific details in the cavity shape for an actual design need to be studied using numerical methods. We have performed simulations with the MAFIA and CST MICROWAVE STUDIO® codes which solve Maxwell's equations on a grid in space, while

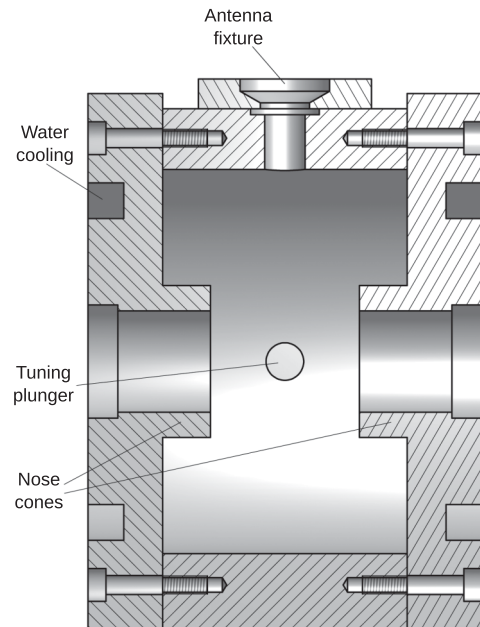


FIG. 3. A cross-section view of the beam current monitoring cavity (created with AUTODESK® INVENTOR®).

respecting boundary conditions and material properties [10]. The numerical solution provided the resonant frequencies and field maps of a requested number of eigenmodes. In further postprocessing steps more details on each mode can be evaluated.

The basic design of the cavity dedicated to beam current measurements foresees a hollow, cylindrical barrel which is closed by two cover plates, as shown in Fig. 3. In case of the pair of position cavities bound to be installed close to each other, two cuplike aluminum bodies are screwed together bottom to bottom. Again, two cover plates complete the setup, Fig. 4 shows some details of the construction. Beam port openings of 34 mm diameter have been included in all cavities, to allow the passage of the beam.

#### 1. Eigenmode frequency

We choose to operate the cavity beam position monitor (BPM) on the third harmonic of the bunch frequency, corresponding to the accelerator frequency of 499.67 MHz. Based upon numerical results, a given resonator geometry was optimized accordingly. Our choice appears to be a good compromise between physical size [compare (1), dependency on the cavity radius] and achievable signal strength. If the TM<sub>110</sub> eigenfrequency would have been tuned to the fundamental bunch

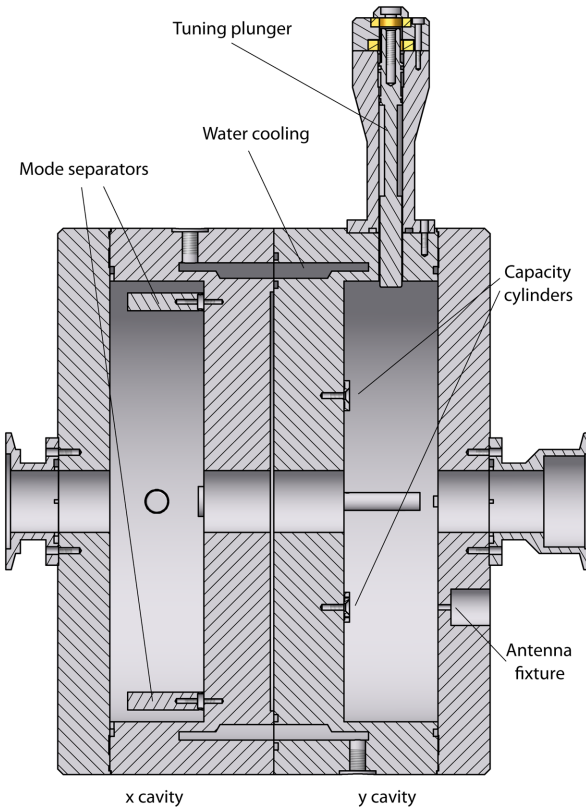


FIG. 4. A cross-section view of the resonator assembly designed to measure the beam position (created with AUTODESK® INVENTOR®).

harmonic, the position cavities would have exceeded 700 mm in diameter. When comparing the actual choice to that case, the excitation strength of the beam (reflected in the bunch factor  $B$  discussed above) and the cavity's shunt impedance (transformed according to geometric scaling laws) find themselves to be reduced by roughly 30% and 40%, respectively. These disadvantages are compensated to some extent by reduced cost and space requirements given by a compact resonator of 244 mm diameter. In order to further reduce expenditures, 3D-forged AlMg 4,5 Mn rather than oxygen-free high-conductivity (OFHC) copper was used as a material.

The current monitor has been designed around the  $\text{TM}_{010}$  mode whose eigenfrequency, as a matter of principle, always has a lower value than the  $\text{TM}_{110}$  dipole mode. Again, operating at the 3rd harmonic of the accelerator rf leads to a cavity diameter of 129 mm. As of this compact dimension, the resonator could be installed roughly 1 m downstream the extraction of the storage ring. For the beam current monitoring cavity, we used OFHC copper, which has a substantially higher conductivity (58 MS/m), compared to the aluminum alloy (18 MS/m) used to manufacture the BPM cavities. This results in a higher  $Q$  value, and therefore a larger output signal.

## 2. Geometry details

Since the  $\text{TM}_{110}$  mode features a dipole structure, care had to be taken to fix its polarization along the transverse axis to be measured. For horizontal/vertical beam position measurements, the beam excited field distributions inside the two BPM resonators are preferable orthogonal oriented, i.e., under 90°. In order to ensure the desired orientation, two mode separating cylinders have been installed symmetrically about each resonator's axis and close to its rim. They detune the eigenmode frequency of any dipole mode polarization not orthogonal to their connecting line. The cross-section view in Fig. 4 shows the two BPM cavities with all details.

To extract the position signal, a fixture for a coupling antenna has been foreseen in the cover caps of the resonators. A location of maximum electric field strength has been chosen, based on the analytical evaluation of an ideal cylinder. As (7) shows, the radial dependency of the transverse E-field is modified by a first order Bessel function, its maximum is located at 0.48 times the cavity radius  $R$ .

Since the antenna axis matches the orientation of the electric field vectors, a signal can be extracted. On each cavity bottom, exactly opposite to the coupling antennas, small *capacity cylinders* have been mounted in order to slightly concentrate the field lines in their vicinity. They allow one to fine-tune resonant frequency and output signal coupling. For symmetry reasons, two of them are mounted in both of the resonators.

In order to optimize the field distribution of the  $\text{TM}_{010}$  mode used in the current measurement cavity,

so-called *nose cones* have been foreseen on both cover plates. As shown in Fig. 3, the cavity walls are locally raised in the form of a cylinder barrel of about 15 mm length, thus prolonging the beam pipe into the resonator. In its vicinity, the concentration of the electric field lines is increased, resulting in higher levels of the output signal.

In order to be able to fine-tune the resonant frequency of the resonators to the third harmonic of the accelerator rf, metallic tuning plungers are mounted on each of the three cavities' barrel. Their shaft rotates in a thread, thus allowing one to vary the depth by which they protrude into the resonator's hollow interior. The more the latter will decrease in volume, the higher its resonant frequencies will be. By virtue of the choke design featured by the position cavities' plungers, disturbances caused by reflections are avoided.

To ensure long-term stable operation in the presence of drifts of the ambient temperature, ducts for water cooling have been included in the mechanical design of all resonators. In the present setup, a feedback loop allows the water temperature to be stabilized within ±0.2 degrees celsius. This limits frequency shifts to roughly ±7 kHz in the case of the aluminum resonators and ±5 kHz in the case of the copper cavity.

## 3. Coupling antennas

The coupling device of the cavity-type BPMs consists of a vacuum tight SMA flange with a gold-plated antenna of 26 mm length soldered to the inner conductor. By fine-tuning the length of the pin antenna, the source impedance of the resonator can be adjusted to the desired 50 Ω, thus matching the wave impedance of the coaxial cables employed for signal transport. In the ideal case, the ratio of source and load impedance, sometimes noted as the coupling factor  $\kappa$ , is one. Considering (2), this case relates to the maximum amount of energy transferred into the external circuitry. There, the signal has to be demodulated with a narrow enough bandwidth for an acceptable signal-to-noise ratio to be obtained. In the present system, coupling coefficients close to 0.9 have been achieved, which is different from the ideal value of one because of tolerances of the pin length.

Considering the  $\text{TM}_{010}$  mode in the intensity cavity, only the maximum value of the magnetic field component is easily accessible. Hence, a wire loop was installed in an opening located on the cavity rim. Since typical signal strengths exceed the average position signal level by a few orders of magnitude, some losses could be tolerated by choosing a coupling coefficient of  $\kappa \approx 3$ . This results in a broadening of the resonance curve, and therefore reduces the dependency of the signal level on frequency drifts, e.g., caused by temperature changes.

Tables I and II list the main parameters of the intensity and position cavities. In case of the latter, the

TABLE I. Parameters of the intensity cavity.

Parameter	Value
Mode	TM <sub>010</sub>
Inner diameter	129 mm
Inner length	82 mm
Opening diameter	34 mm
Resonant frequency $\nu_0$	1.499010 GHz
Shunt impedance $R_s$	1.05 MΩ
Unloaded quality factor $Q_0$	11900
Coupling factor $\kappa$	3.0

TABLE II. Parameters of the  $x$ -position cavity.

Parameter	Value
Mode	TM <sub>110</sub>
Inner diameter	242 mm
Inner length	52 mm
Opening diameter	34 mm
Resonant frequency $\nu_0$	1.499010 GHz
Shunt impedance $R_s/\Delta x^2$ (CST)	411 Ω/mm <sup>2</sup>
Unloaded quality factor $Q_0$	11090
Coupling factor $\kappa$	0.89

characteristics of the  $x$  resonator are given as an example. The shunt impedance of the current cavity has been determined by means of a bead-pull measurement. In the case of the position cavities, we rely on the numerical results computed by CST MICROWAVE STUDIO®. The practical achieved values may stay a few percent below these numbers due to manufacturing and contact imperfections.

Inserting the respective parameters into (2) allows for a reasonably good estimate of the scaling factor between measured signal voltage and beam parameter to be determined. Nevertheless, measurements performed by additional diagnostics installed in the beam lines allow for direct empirical calibration. Thus, uncertainties of the parameters and drift effects occurring due to temperature changes can be compensated.

### III. DEMODULATION OF THE CAVITY SIGNALS

#### A. Logarithmic amplifier for demodulation of the beam current signal

The current monitoring cavity will output signal levels ranging 5–75 fW, equivalent  $-113$  to  $-101$  dBm, assuming typical beam currents of 200–800 pA. In an rf front end, located close to the storage ring tunnel, the signal is preamplified by about 90 dB and then mixed down to an intermediate frequency (IF) of 180 MHz, suitable for the signal detection using a logarithmic amplifier. Appropriate bandpass filtering at both, the rf and the IF stages, allows for the removal of potentially disturbing signal components.

The output signal of the logarithmic amplifier is subjected to low-pass filtering with the cutoff at a few Hz. It is then fed to an optical converter in order to be transferred via a glass fiber of some 15 m length to a receiver. The latter is installed in close proximity to a custom VME computer board, used for the digital signal processing. It features a 12-bit bipolar analog-to-digital converter driven at 100 Hz sampling rate. The signal voltage to beam current conversion is performed in a C-routine, based on an empirical factor. It was determined by dumping the entire electron beam over one extraction cycle into a well-calibrated Faraday cup located in one of the experimental areas.

#### B. Phase-sensitive detection of the position signals

In the case of the position measurement, the use of lock-in techniques to detect the cavity signals has been demonstrated to be very successful [4,5]. Lock-in amplifiers can separate very weak signals from noise in case their frequency is precisely known. Since we are expecting low-power position cavity signals in the proximity of a well-defined resonant frequency and competing with noise, we chose this approach to signal demodulation.

##### 1. Basic concept

Figure 5 shows a simplified schematic of the digital lock-in amplifier (SR830, by Stanford Research Systems, Inc.) used in our application [11]. It internally multiplies two signals, a fairly strong and clean reference signal (Ref.) used to excite an experimental setup, and the resulting measurement signal (Sig.), much weaker and overlayed by noise. The product will include a sum of terms of the following shape:

$$U_{\text{out}} \propto U_{\text{ref}} U_{\text{sig}} \cos[(\omega_{\text{ref}} - \omega_{\text{sig}})t + \phi]. \quad (8)$$

Only the signal component matching the reference frequency will result in a DC signal in the output of the so-called *phase-sensitive detector* (PSD). The wanted signal components, known to lie very close to the reference frequency  $\omega_{\text{ref}}$ , will result in very slowly oscillating terms. By employing low-pass filters, an output signal roughly proportional to the amplitude of the wanted signal remains,

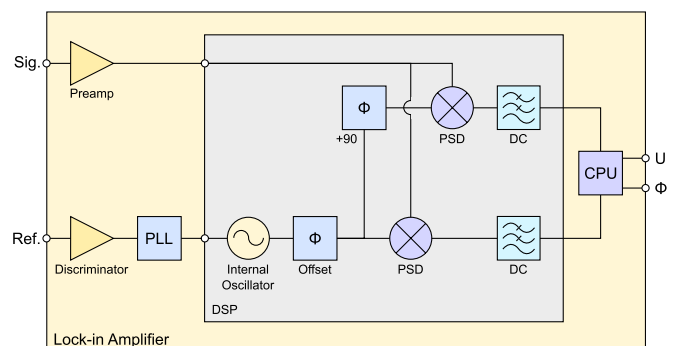


FIG. 5. Simplified block schematic of the SR830 lock-in amplifier [11].

reduced by the cosine of the phase difference between reference and input.

In our application, the master rf generator driving the accelerator systems provides the reference signal. Since the beam's time structure is directly related to the accelerating voltage, the cavity signals excited by the particle bunches will be linked in frequency and phase to the accelerating rf oscillations. The diagnostic cavities are tuned to their third harmonic. Consequently, the generator signal has to be tripled in frequency in order to be used as reference.

The stable phase relationship between cavity and reference signal is used to detect the “cavity half” (lower or upper, left or right), which was passed by the beam. The sign of the electrical field strength of the  $\text{TM}_{110}$  mode flips when crossing the  $xz$ , respectively  $yz$ , symmetry plane of the cavity, thus resulting in a phase shift of 180 degrees in the output signal.

In the setup presented here, the dual channel feature of the lock-in amplifiers in use was essential to determine the phase  $\phi$  in (8). As shown in Fig. 5, a second multiplication is performed in addition to the already explained demodulation procedure, but with the reference signal shifted in phase by 90 degrees. The amplifier thus obtains both the  $I$  and  $Q$  components of the acquired signal. Therefore, it can directly compute their vector sum, the signal magnitude  $U$ , and the phase  $\phi$  of the signal in relation to the reference. This scheme, in contrast to a single channel design, allows one to demodulate stable baseband output signal magnitudes and phases, even if input and reference frequencies are not in phase. The measured data is read out via an

IEEE-488 interface (GPIB) to a PC running Linux and equipped with an appropriate interface card.

## 2. Frequency down-conversion

The digital lock-in amplifiers accept only signals with an upper frequency content of 102 kHz, therefore the 1.499010 GHz dipole mode signals (rf) need to be down-converted to an *intermediate frequency* (IF) of typically 90 kHz using analog frequency mixing. A voltage controlled oscillator provides the *local oscillator* (LO) signal fed into the double balanced mixers. By adjusting the tuning voltage via feedback loop, temperature induced changes in the output frequency can be compensated for. In order to maintain the integrity of the phase relation, a power divider distributes the oscillator signal to both the reference and the cavity signal paths.

In practice, the reference signal needs to be well isolated from the beam signals, even a tiny cross talk will generate unwanted reference signal components in the position signal path, causing an artificial beam offset. Four circulators (isolation of  $-23$  dB each) have consequently been integrated in the LO signal path leading to the mixer assigned to the reference signal, thus dampening its propagation into other parts of the rf circuitry [5]. Figure 6 shows a complete block diagram of the rf signal processing.

## 3. Filtering, shielding, and mass separation

As shown in Fig. 6, the output of all active components in the circuitry, namely the frequency multiplier and the

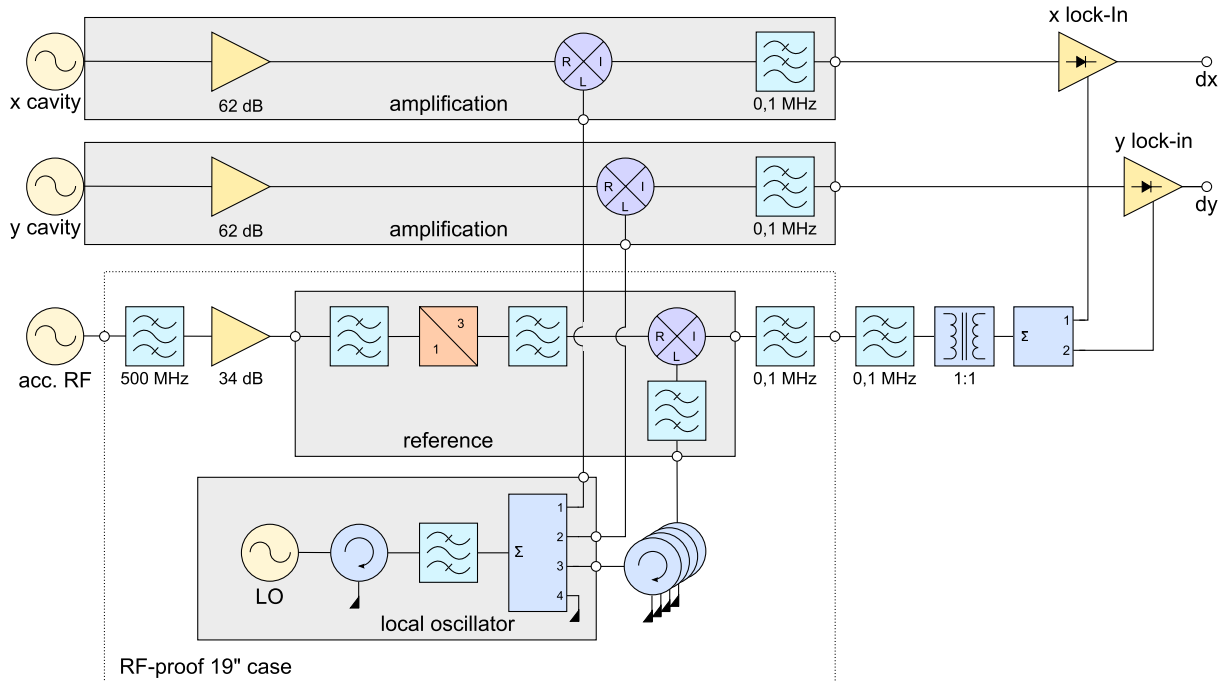


FIG. 6. Scheme of the rf signal processing. The shaded areas note functional units assembled in dedicated, well shielded rf housings. The rf, LO, and IF ports of the mixers are designated by first letters.

local oscillator, as well as the reference signal obtained from the master generator, are fed into bandpass filters in order to remove spurious signals. The signals from the mixers outputs are sent through low-pass filters, thus dampening frequency components exceeding the lock-in amplifier's upper frequency limit of 102 kHz.

Even with these filtering efforts, we did not reach the required performance of the system due to electromagnetic interference between some components. Consequently, more efforts on shielding and the optimal location of components had to be made, e.g., separating low level signal components from those processing higher rf signal levels. A module dedicated to the preamplification (by  $\approx 62$  dB) and frequency mixing of the cavity signals has been directly mounted to each of the position cavities. By virtue of the water cooling administered to the latter, they represent a heat sink effectively dissipating the thermal power issued by the amplifiers. The components included in each of the modules are enclosed by shaded rectangles in Fig. 6.

The dedicated modules for processing the reference signal, as well as for providing the local oscillator signals, are gathered with a few other parts into a well shielded rf housing, as shown by the dashed line in Fig. 6. This unit is installed in a 19 inch rack close to the position resonator compound, together with the lock-in amplifiers and the PC used for readout purposes.

#### IV. PC SYSTEM FOR DATA READOUT AND CONTROL

##### A. PC hardware

In order to communicate with both, the lock-in amplifiers to demodulate the position signals, and the accelerator control system, a dedicated PC has been set up. It runs a Red Hat Linux distribution (Version 9) as operating system which had proven to be compatible with the drivers of the PCI cards to be installed. The lock-in amplifiers are controlled via a GPIB interface, the control voltage for the LO is provided via a 12-bit D/A board.

##### B. Measurement software

In order to be able to provide position values for display within the accelerator control system, a C++ program has been written to process the signal voltages provided by the lock-in amplifiers. Since the position signal has to be normalized, beam current values are read out via Ethernet from the VME computer processing the respective signals. Additionally, the software has to manage several control loops, needed for the position measurement.

##### 1. Frequency and phase control

Both the IF signals and the phase relationship between reference and cavity signal are prone to temperature drifts.

With an LO frequency of roughly 1.498920 GHz fed to the mixers, the day/night temperature variation alone has been observed to result in a frequency shift of up to 30 kHz. Since the resulting intermediate frequency could possibly exceed the frequency acceptance limit of the lock-in amplifiers, a feedback loop has been set up. The amplifiers provide a reading of the actual reference frequency, thus giving an indication for readjustment of the voltage controlled LO. A change of one bit at the D/A card output results in a shift of approximately 4 kHz in the oscillator frequency. The control loop routine detects and compensates for such deviations from the nominal value of 90 kHz, specified in the control system menu.

In addition, the phase difference between cavity and reference signal is checked in regular intervals. Thermal drifts may lead to deviations from the nominal values of  $+90^\circ$  and  $-90^\circ$ , each related to one polarity of the beam's displacement, respectively. As indicated in Fig. 5, the lock-in amplifiers do allow for an offset to be added to the measured phase relation, thus facilitating the necessary adjustments.

##### 2. Sample rate

The query processing speed of the lock-in amplifiers limits the sampling rate to approximately 9 Hz in the current setup. The position signal provided by the lock-in amplifiers has to be normalized to the beam current. This is performed by polling the beam current values via Ethernet from the signal processing VME board, at the same rate the voltages of the lock-in amplifiers are read out.

#### V. PERFORMANCE OF THE MEASUREMENT SYSTEM

##### A. Time resolution

The maximum lock-in amplifier readout rate gives  $\sim 30$  data points for the entire slow-spill extraction period of typically four seconds. Drifts of the beam position can

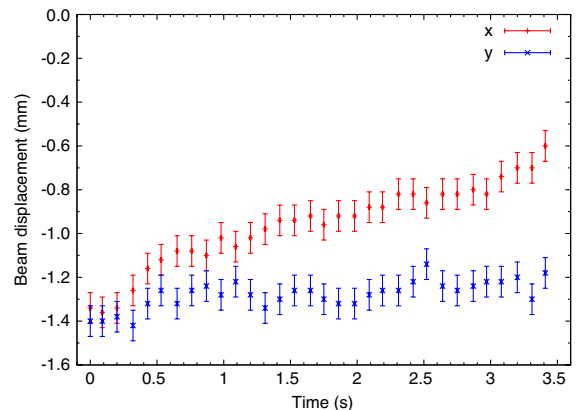


FIG. 7. Typical beam position data from the cavity BPM system, at a beam current of 280 pA. Each data point averages the position readings of ten resonance extractions.

thus be resolved in time, as shown in Fig. 7. They predominantly occur in the horizontal axis, which is due to small imperfections of the 3rd integer resonance extraction scheme. The actual reactivity of the position measurement depends on the low-pass filter settings.

### B. Position resolution

The noise at the output of the lock-in amplifiers notably depends on the *time constant*  $\tau$  chosen for the low-pass filtering of the PSD output signals. Since up to ten time constants (in case of four filter stages) have to elapse for input changes to be accurately (by 99%) reflected at the output, noise can only be reduced at the cost of reaction speed. A good compromise between noise and speed has been established empirically for our setup, i.e., setting the global time constant which is valid for each of the four active filter stages, to 30 ms.

To evaluate the performance of the position measurement, the displacement in the  $x$  and the  $y$  direction is plotted against typical beam current values in Fig. 8, each data point representing the average over one extraction cycle. The mechanism used to vary the external beam current leads to slight position deviations from cycle to cycle. Activating a beam current stabilization feedback, the relative position can be determined with a resolution of at least  $\sim 50 \mu\text{m}$  for beam currents  $> 100 \text{ pA}$ . The residual noise however limits the position measurement near the cavity symmetry axis. At a typical beam current of 250 pA, beam displacements of  $< 120 \mu\text{m}$  cannot be detected.

In order to give a more general estimate for the theoretical measurement resolution, we relate the distance  $\Delta x$  between two discernable position readings ( $x_0, x_1$ ) to the respective signal power difference  $\Delta P$ . According to the proportionality in (2), we postulate

$$\Delta P = f(x_1^2 - x_0^2) \quad (9)$$

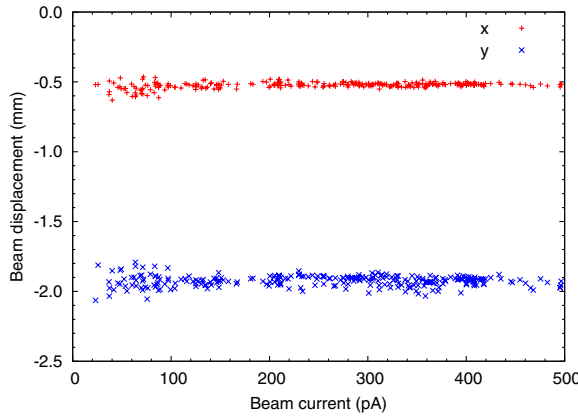


FIG. 8. Averaged beam position data vs beam intensity. Some of the scattering above 100 pA is mostly due to unstable beam extraction conditions. At low beam currents, resolution and reproducibility of the position measurement is limited due to noise and other imperfections.

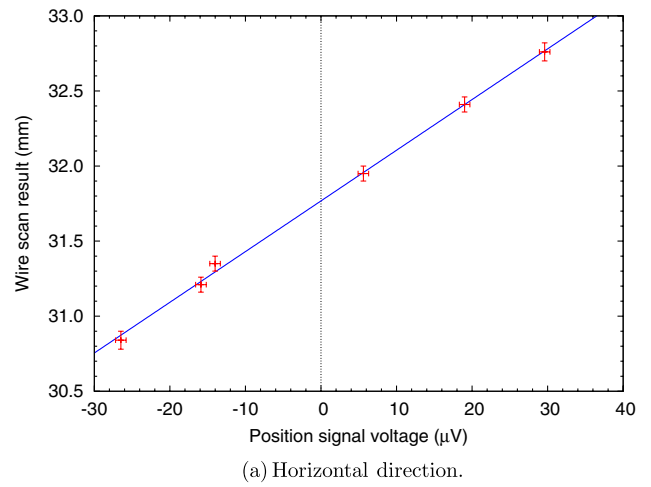
while introducing the scaling factor  $f$ . This gives

$$\Delta x = \frac{\Delta P}{f(2x_0 + \Delta x)} = \frac{0.014 \text{ mm}^2}{2x_0 + \Delta x}, \quad (10)$$

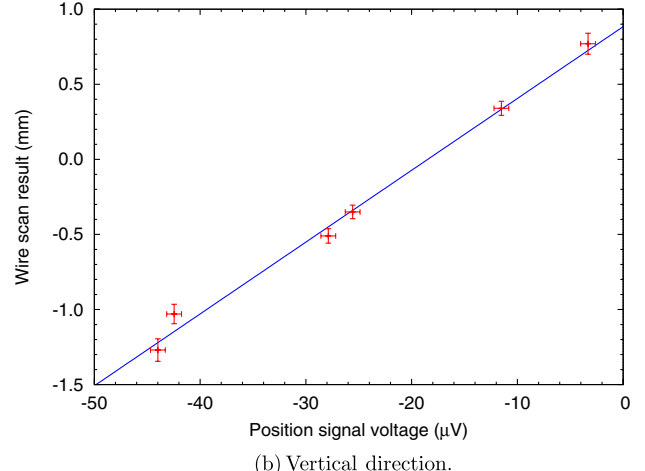
the last equality holding for the above stated lower detection limit ( $x_0 = 0$ ) at a beam current of  $\sim 250 \text{ pA}$ . With the beam displaced by a millimeter, an estimate of the theoretical resolution gives  $\sim 7 \mu\text{m}$ . Practical measurements suffer from slightly varying conditions of the extraction mechanism.

### C. Stability of the reported absolute beam position

Wire scan measurements performed inside the CBELSA/TAPS experiment's radiator target setup allow for an empirical calibration of the measurement system. Figure 9 illustrates the result of a typical calibration run, performed for the horizontal and the vertical axis. The absolute measurement precision is limited by the wire scan accuracy.



(a) Horizontal direction.



(b) Vertical direction.

FIG. 9. Calibration of the position measurement by comparing the signal voltages with wire scan results, performed at a beam current of 800 pA.

While the calibration stability has proven satisfactory for typical experimental data taking runs of a few weeks, we observe long-term effects on the reported absolute beam position. It typically varies by a few percent over some months, likely due to temperature-related drifts in the rf circuits as well as in the resonant frequency of the cavities. While the water cooling provides for some stability of the latter, smaller frequency drifts of some 10–20 kHz cannot be prevented, with the result of variations in the position signal levels. Possible strategies to compensate for these long-term drift effects are under investigation.

## VI. CONCLUSION

The concept of a beam position measurement based on cavity BPMs, utilizing a phase-sensitive detection scheme, was successfully adapted. The high sensitivity allows the on-line monitoring of the beam position in the external beam line of the ELSA facility for electron beam currents well below 1 nA. The typical resolution of 50  $\mu\text{m}$  surpasses the requirements of the experiment. Means to normalize the position signals are provided by an additional cavity for current measurements. The data acquisition rate of 9 Hz allows for the time-resolved detection of position deviations during standard operation, enabling the implementation of corrective feedback loops.

## ACKNOWLEDGMENTS

The experience gathered at the Institute for Nuclear Physics at the Johannes Gutenberg University Mainz, Germany, was generously shared with us and helped in optimizing the general cavity design. Namely, Peter Jennewein gave us valuable input regarding the phase-

sensitive detection scheme. Dr. Steffen Schumann was helpful with the antennas' assembly. In addition, we would like to thank the CBELSA/TAPS collaboration for providing the wire scan readings. Finally, we gratefully acknowledge the funding of the project by the DFG within the SFB/TR 16.

- 
- [1] W. Hillert, *Eur. Phys. J. A* **28**, 139 (2006).
  - [2] U. Thoma (CBELSA/TAPS Collaboration), *AIP Conf. Proc.* **1257**, 173 (2010).
  - [3] H. Schmieden, *Int. J. Mod. Phys. E* **19**, 1043 (2010).
  - [4] R. Ursic, R. Flood, C. Piller, E. Strong, and L. Turlington, in *Proceedings of the Particle Accelerator Conference, Vancouver, BC, Canada, 1997* (IEEE, New York, 1997), Vol. 2, pp. 2131–2133.
  - [5] H. Euteneuer, H. Herminghaus, P. Jennewein, K.-H. Kaiser, H.-J. Kreidel, D. Mittwich, G. Stephan, T. Weis, and P. Zinnecker, in *Proceedings of the 1992 Linear Accelerator Conference, Ottawa, Ontario, Canada, 1992* (AECL Research, Chalk River, Ontario, 1992), Vol. 1, pp. 356–358.
  - [6] R. Lorenz, *AIP Conf. Proc.* **451**, 53 (1998).
  - [7] S. Lee, *Accelerator Physics* (World Scientific, Singapore, 2004).
  - [8] H. Wiedemann, *Particle Accelerator Physics* (Springer, New York, 2007).
  - [9] A. Chao and M. Tigner, *Handbook of Accelerator Physics and Engineering* (World Scientific, Singapore, 1999).
  - [10] T. Weiland, *Archiv Elektron. Uebertragungstechnik* **31**, 116 (1977).
  - [11] Model SR830 DSP Lock-In Amplifier, Stanford Research Systems, 1290-D Research Avenue, Sunnyvale, California (2011), revision 2.5.